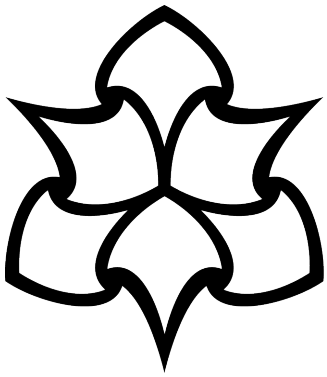

Diagnosis of the Hypopnea syndrome in the early stage

Xiaodong Yang[1] · Dou Fan[1] · Aifeng Ren[1] · Nan Zhao[1] · Syed Aziz Shah[1] · Akram Alomainy[2] · Masood Ur-Rehman[3] · Qammer H. Abbasi[4]

Abstract
Hypopnea syndrome is a chronic respiratory disease that is characterized by repetitive episodes of breathing disruptions during sleep. Hypopnea syndrome is a systemic disease that manifests respiratory problems; however, more than 80% of Hypopnea syndrome patients remain undiagnosed due to complicated polysomnography. Objective assessment of breathing patterns of an individual can provide useful insight into the respiratory function unearthing severity of Hypopnea syndrome. This paper explores a novel approach to detect incognito Hypopnea syndrome as well as provide a contactless alternative to traditional medical tests. The proposed method is based on S-Band sensing technique (including a spectrum analyzer, vector network analyzer, antennas, software-defined radio, RF generator, etc.), peak detection algorithm and Sine function fitting for the observation of breathing patterns and characterization of normal or disruptive breathing patterns for Hypopnea syndrome detection. The proposed system observes the human subject and changes in the channel frequency response caused by Hypopnea syndrome utilizing a wireless link between two monopole antennas, placed 3 m apart. Commercial respiratory sensors were used to verify the experimental results. By comparing the results, it is found that for both cases, the pause time is more than 10 s with 14 peaks. The experimental results show that this technique has the potential to open up new clinical opportunities for contactless and accurate Hypopnea syndrome monitoring in a patient-friendly and flexible environment.

Keywords Hypopnea syndrome · Respiration sensor · Early warning · Biomedical engineering · Machine learning

1 Introduction

Sleep is an essential survival skill and has great significance to human health. Sleep not only affects the productivity and physical vitality of a person but is also related to many diseases including diabetes, depression, and even stroke and heart failure [1]. Therefore, sleep function monitoring has a high medical value.

✉ Xiaodong Yang
xdyang@xidian.edu.cn

[1] School of Electronic Engineering, Xidian University, Xi'an 710071, Shaanxi, China

[2] School of Electrical Engineering and Computer Science, Queen Mary University of London, London E1 4NS, UK

[3] School of Computer Science and Electronic Engineering, University of Essex, Colchester CO4 3SQ, UK

[4] School of Engineering, University of Glasgow, Glasgow G12 8QQ, UK

Hypopnea syndrome is a common illness that occurs when throat muscles intermittently relax and block the airway during sleep [2]. It is characterized by repetitive episodes of shallow or paused breathing during sleep and is usually associated with a reduction in blood oxygen saturation. These episodes of paused breathing typically last 20–40 s. Signs and symptoms of sleep apnea include excessive daytime sleepiness, loud snoring, and breathing cessation during sleep, abrupt awakening due to respiratory disorders, such as hypopneas, apneas, and choking. Back in the days, Hypopnea syndrome was considered as a sleep habit accompanied by snoring, but it is now regarded as a serious clinical disorder. Several studies indicate that a high percentage of patients suffering from Hypopnea syndrome remain unidentified, which can greatly affect their routine life and might create severe health complications, such as reduced work performance. Furthermore, evidence suggests that Hypopnea syndrome is related to systemic diseases, such as cardiovascular diseases (e.g., (1) coronary disease is due to the angiosclerosis and the blood cannot

flow properly; therefore, the red blood cells cannot transport oxygen and there is not enough oxygen for the cardiac muscle; (2) angina; (3) cor pulmonale, it leads to the hypertrophy of right ventricular; (4) hypertension; (5) hyperlipidemia; (6) hyperglycemia, etc.) and glucometabolic impairments (it is necessary to keep the blood glucose at certain level, and this task is mainly fulfilled by the liver) as well, as various pediatric complications, such as psychological and behavioral disorders, nocturnal enuresis, and growth-related disorders [3]. Greater association with Hypopnea syndrome not only brings cardiovascular problems and neurological disorders; it can also cause sudden death in case of severe breathing obstruction [4]. Timely detection of Hypopnea syndrome through observation of respiratory disorder episodes therefore has vital importance in personal healthcare.

Polysomnography (PSG) is a standard method for the diagnosis of Hypopnea syndrome. It is based on a comprehensive recording of biophysiological changes that occur during sleep. The test is typically a full-night study performed on a patient in a laboratory environment by medical experts. The PSG monitors heart, lungs and brain activities, breathing patterns, arm and leg movements, and blood oxygen levels in the form of electroencephalogram (EEG), electrocardiogram (ECG), electrooculogram (EOG), electromyography (EMG), and oxygen saturation (SpO_2). Though Hypopnea syndrome can be objectively assessed and monitored by these signals, the subjects are often uncomfortable by deploying electrodes and wearing bands on their bodies during this long procedure. Moreover, the data can only be obtained in institutions or hospitals equipped with dedicated devices [4].

Various approaches have been applied to achieve sleep apnea [5–9] detection: in [5], the apnea–hypopnea events are detected via an alternative sensor, and the new algorithm has been developed to find the sleep-disordered breathing from the RIP-sum signal; in [6], SpO_2 signals were considered in the SAHS classification, and advanced algorithms are used to extract key information; Villar et al. [7] found that AdaBoost is helpful in enhancing the diagnostic ability of oximetry signal; in [8], heart rate signals are used to detect sleep, and accurate results are obtained by using classifier; in [9], hypoglossal nerve stimulation is used in the treatment of obstructive sleep apnea, and the OSA is defined by citing its facts, effects, and treatments. Going through all these recent works, although various approaches and indicators have been considered, it is noticeable that limited research has been done on the noncontact detection using wireless signals. It is also worth mentioning that alternative physiological signals were used to overcome the drawbacks of polysomnography [10–12]. One of the examples includes spectral analysis of snoring sounds to detect Hypopnea syndrome [12].

With the recent developments, wireless sensing has opened the doors for sleep monitoring systems leveraging various sensors, such as audio, image, force, and temperature [13–22]. Most of these wireless systems are contact-oriented and require wearable sensors worn by the patient to acquire adequate precision levels in a clinical setting. Use of smartphones accelerometer and audio recordings to monitor sleep disorders is proposed in [13–15]. Behar et al. [14] studied a wearable system composed of an armband sensor, a face-worn microphone, and a wrist-worn oximeter connected to the smartphone for the sleep apnea detection. Force sensors deployed under the mattress top have also been used to detect the heart rate, sleep pattern, snoring, or respiration rate [16–20]. Martinez et al. [21] investigated a wireless sensor system to detect respiratory rate using received signal strength indicator. This system requires 15–20 sensor nodes to achieve high classification accuracy. Video recordings of sleep patterns through camera-based optical approach are adopted, to detect the breathing pattern via video recordings is discussed in [22, 21]. Cost-effectiveness of polysomnography technique using split-night sleep monitoring is considered in [23]. Though wearable technologies have emerged as a potential solution to monitor the patients unobtrusively, outside clinical settings, they limit patients comfort due to requirement of a number of body-worn sensors; on the other hand, the potential patients have the consciousness that they are being monitored and may control their physiological activities through consciousness.

In this paper, we investigate a noninvasive system based on S-band sensing to monitor the sleep apnea. The novelty of this work lies in the development of an accurate and efficient monitoring technique that provides continuous, contactless, and patient-friendly solution. The privacy of the patients can be protected as well. Usability and accuracy of the proposed system are established through a comparative study with standard commercial respiratory sensors.

2 System design

The proposed method primarily uses sensing technique that works at S-band. Details of the system architecture are discussed in this section.

2.1 Basic system architecture

The proposed sensing system makes use of a wireless link between two antennas positioned at two sides of the human subject, as illustrated in Fig. 1. The two antennas are placed around the chest and are visually in a straight line, enabling them to establish a line-of-sight (LOS) link. The

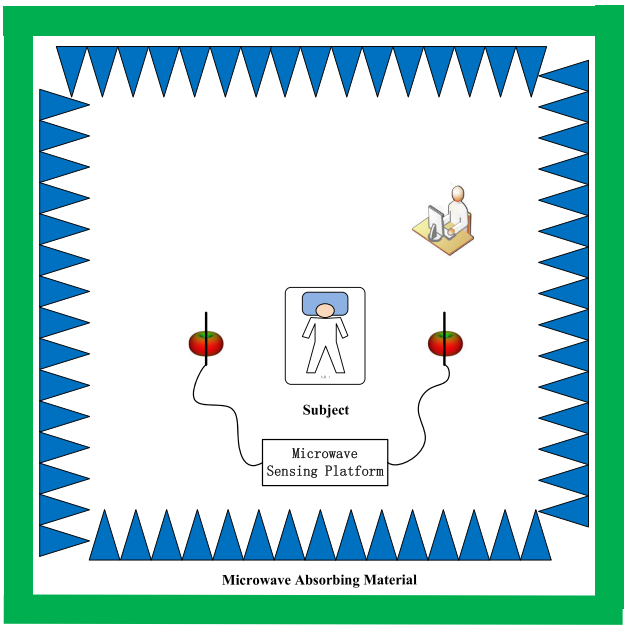

Fig. 1 Experiment setup for detecting sleep apnea

distance between the two antennas is kept at 3 m to replicate a typical patient monitoring system in a wireless environment with sample rate of five packets per second.

This sensing platform is an in-house system and consists of a spectrum analyzer (E8600), vector network analyzer (Agilent E8363B), antennas, software-defined radio, RF generator, and desktop workstation equipped with network adaptor. The measurement setup of this sensing platform is shown in Fig. 2. This system can work at a number of frequencies depending on the operating band of the antennas. For our work, we have selected the S-band frequencies of 2 GHz–4 GHz due to their wide usage in healthcare applications and added benefits discussed in the proceeding section.

The system employs monopole antennas, which are off-the-shelf, at the transmitting and receiving ends. This selection of the antennas is based on a twofold approach, making the system universal by using widely available standard type of antennas and decreasing the antenna's effect on the sensitivity of the system. Along with the antenna, the emitter includes RF generator, coaxial cable, and connector. It is also worth mentioning that the current system and algorithm framework are feasible for single-subject detection, and for multiple patients' scenarios, more complicated algorithm frameworks have to be proposed; also, background noise and environmental interference have also to be decreased through the application of advanced algorithms.

The propagation mechanism of RF signals between the transmitter and receiver is complex and can take both line-of-sight (LOS) and non-line-of-sight (NLOS) paths, as shown in Fig. 3. The LOS path refers to the signals propagating in a direct path without any blockage by the human subject. The walls of the room are covered with RF absorbing material to get rid of these scattered components. It not only simplifies the overall system model but also improves the accuracy through better detection of minute chest movements due to breathing and accompanying spatial changes in the channel response.

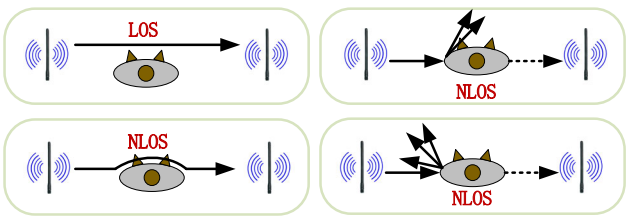

Fig. 3 Radio propagation modes for sleep apnea detection

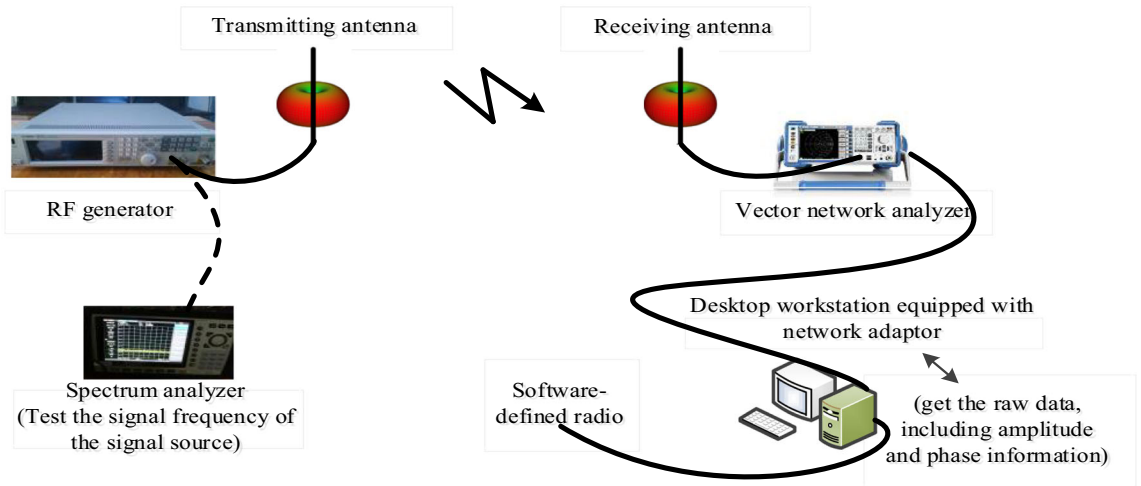

2.2 Wireless channel information at S-band

The proposed system observes the wireless channel between the transmitter and receiver and notes down the sudden variations as a result of change in breathing pattern to detect the sleep apnea episodes. The transmitter and receiver transmit wireless signals through a spatial data stream. By using orthogonal frequency division multiplexing (OFDM) technology, this data stream is divided into 56 orthogonal channels (called subcarriers) and a group of 30 subcarriers, provided to upper layer users. Therefore, a group of 30 OFDM subcarriers carrying the channel information is used and exported to the user. Each of the exported data packets contains both the amplitude and phase information for a particular subcarrier:

$$H(f_n) = |H(f_n)|e^{j\angle H_n}. \quad (1)$$

where $H(f_n)$ represents the wireless channel information, namely the channel frequency response (CFR) for nth subcarrier at the central frequency, f_n, $|H(f_n)|$ is the amplitude information, and $\angle H_n$ describes the phase response.

The rationale behind using the S-band sensing is based on the argument that the wireless channel information retrieved using S-Band sensing technique is a superior metric as compared to other techniques, such as received signal strength indicator as it presents a fine-grained information of the wireless channel and is more efficient for small-scale multipath fading [24]. The core idea of using wireless channel information is to monitor the breathing pattern of the human subject and identify sleep apnea episodes by keeping track of any minute changes in the channel response. S-band sensing is sensitive enough to record these small changes but the received signal strength indicator only provides the received power levels and fails to note down the effects induced by small chest movements caused by breathing irregularities. Moreover, reflections and scattering of the radio frequency (RF) signal caused by the chest movements affect different subcarriers differently. S-band sensing technique enables examination of each of the subcarriers, while the conventional received signal strength indicator only presents average power that can potentially overlook these small changes.

From each wireless channel information (WCI) packet, a 30×1 matrix in the form of CFR can be extracted. Each row of the WCI matrix describes one subcarrier. If CFR_m represents the channel frequency response of mth packet received, then:

$$\mathrm{CFR}_m = [[h^1(m), h^2(m), h^3(m), \ldots, h^{30}(m),]] \quad (2)$$

where $h^i(m)$ denotes the CFR of the subcarrier i, at time m. To examine the time history of CFR_m, total number of CFR_m recorded at various time intervals are combined and expressed as:

$$\mathrm{CFR} = [[\mathrm{CFR}_1, \mathrm{CFR}_2, \mathrm{CFR}_3, \ldots, \mathrm{CFR}_k,]] \quad (3)$$

Here, CFR is a $30 \times k$ matrix, where k describes the total number of packets received using network adapter and represents the change in the wireless channel over the observed time duration.

2.3 Experimental workflow

The usability of the proposed system is established through performance comparison with a standard respiratory sensor. Thus, the experimental workflow has two main components:

1. Normal breath detection using both the S-band sensing technique and an invasive breathing sensor.
2. Hypopnea syndrome detection through wireless channel information and an invasive breathing sensor.

The respiratory sensor also helps to identify the specific frequency that should be chosen, which is a key step in sleep apnea detection.

Raw wireless channel information recorded by S-band sensing technique is first calibrated and filtered, as shown in Fig. 4. The selective weight median filter is used for data calibration and filtering. The wireless channel information measurements are then examined for changes that occurred due to small chest movements associated with varying breathing pattern. If any changes are recorded, all of the 30 subcarriers are analyzed to look for any abnormalities in the breathing pattern. In case of no sudden disturbances in the breathing pattern due to chest movements, the wireless channel information data would remain constant for the period of observation, inferring an absence of sleep apnea. A comparison between the two datasets would result in the detection of the Hypopnea syndrome.

3 Results and discussion

3.1 Benchmark study

A benchmark study is carried out first to establish the usability of S-band technique for breathing pattern monitoring. In this experiment, six subjects (details as shown in Table 1) volunteered to assess the proposed method. For each experiment, three datasets were collected from each subject (only one set of observations for each experiment from subject 1 is shown in detail in this paper). Figure 5 shows the raw amplitude data obtained using S-band sensing technique for 30 subcarriers over a period of 60 s when the subject was breathing normally. The

Fig. 4 Overall framework and specific workflow for non-contact detection

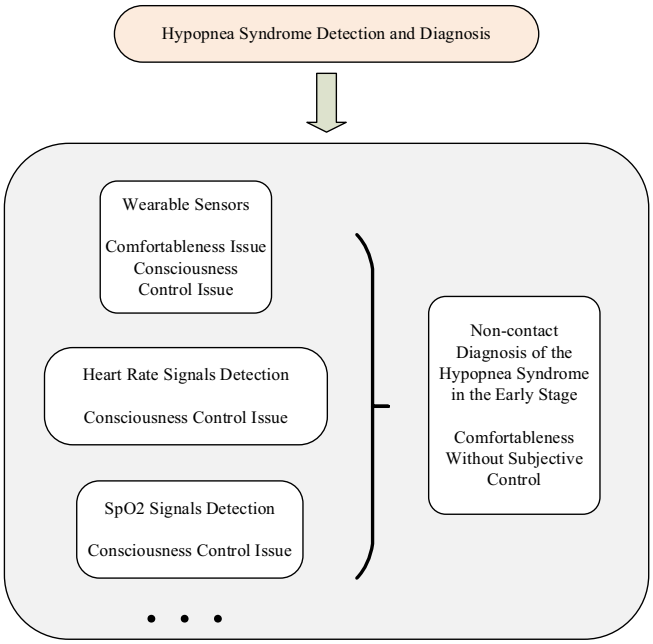

(a) Overall Framework

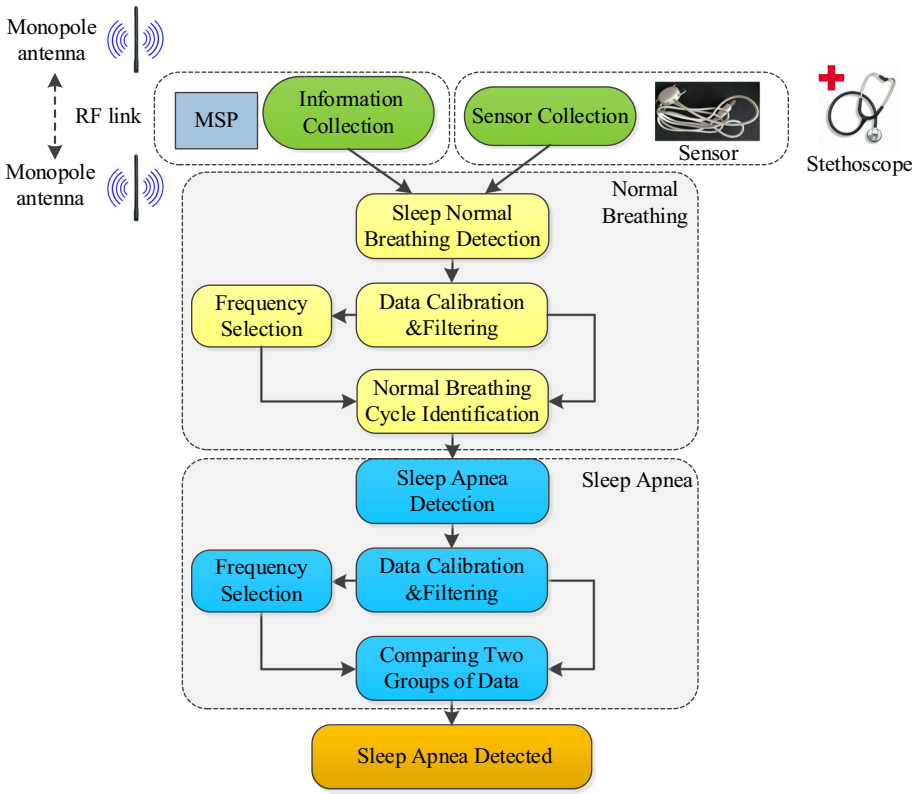

(b) Work flow for non-contact detection

measurements were taken when the patient was lying straight, facing upwards. Clear variances and some wave-like pattern can be observed in the observed data.

To examine the breathing pattern, further processing of the CFR amplitude data is needed. The first step is to perform filtering. Figure 6a shows the raw amplitude of all the 30 subcarriers in 2-D. It can be seen that there are some

Table 1 Details for six subjects

ID	Gender	Weight (kg)	Height (cm)	Hypopnea syndrome	ID	Gender	Weight (kg)	Height (cm)	Hypopnea syndrome
1	Male	75	173.0	No	4	Male	78	176.2	Yes
2	Male	82	180.6	No	5	Male	82	175.9	Yes
3	Female	60	163.4	No	6	Female	62	160.1	Yes

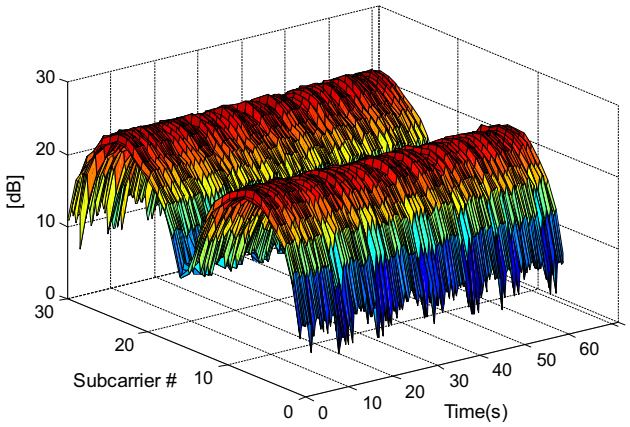

Fig. 5 3-D illustration of the raw data obtained for normal breathing

abrupt changes in all the subcarriers. To track clear breathing behavior, these abrupt change points must be eliminated.

The selective weight median filter is used to remove the abrupt change points. The choice of this filter is based on the fact that it is a highly effective elimination method for the impulse noise [25], appearing in Fig. 6a. The conventional filters like Chebyshev or Butterworth are not appropriate to remove such high-frequency noise as they blur the rising and falling edges of the signal which are critical for identifying the sleep apnea episodes in this study. Figure 6b shows a much cleaner CFR data for the 30 subcarriers after using the selective weight median filtering.

We will now discuss the process of characterizing normal and abnormal breathing. From Fig. 6b, we can see that most of the 30 subcarriers have conspicuous periodic oscillatory patterns correlated with breathing, whereas the rest are messy. The channel giving most clear information of breathing pattern with most obvious wave-like pattern after the filtering process is considered as the most 'suitable' for the detection of the Hypopnea syndrome. Maximum variance approach is applied to select the most suitable subcarrier due to the fact that greater variance corresponds to higher sensitivity. Based on this, we selected the time history of the 26th subcarrier as shown in Fig. 7.

The data for the chosen individual subcarrier are analyzed for a sample of 60 s. Figure 7a shows the normal breathing of a person lying in a straight position. Signs of

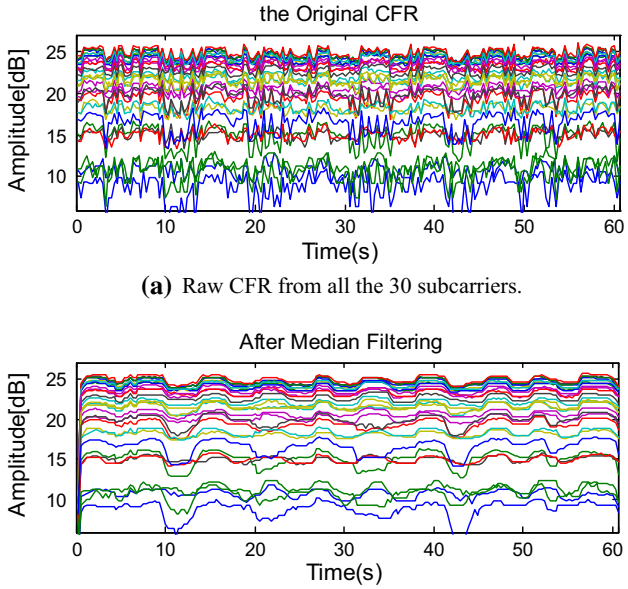

(a) Raw CFR from all the 30 subcarriers.

(b) CFR data after applying selective weight median filtering.

Fig. 6 Variances of 30 sequences of normal breathing. **a** Raw CFR from all the 30 subcarriers. **b** CFR data after applying selective weight median filtering

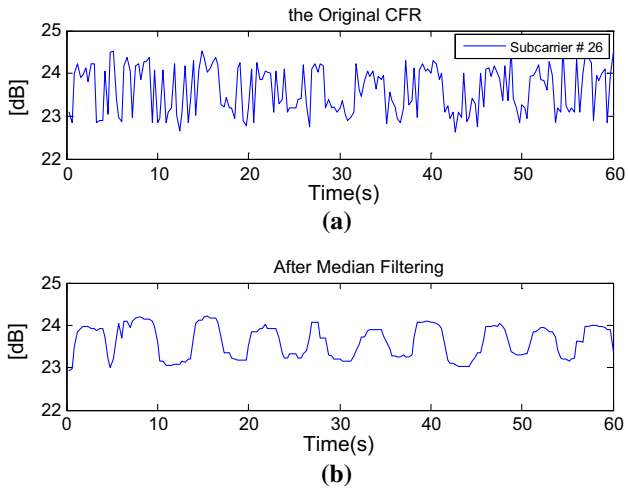

Fig. 7 Time history of the 26th subcarrier and corresponding filtered data for 60 s duration

breathing are clearly evident due to fluctuations in amplitude information. Figure 7b shows the CFR values after applying the median filter.

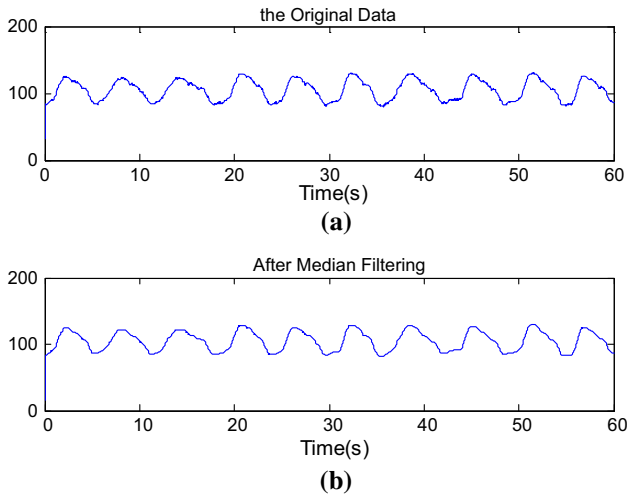

Fig. 8 Normal breathing obtained using breathing sensor

Figure 8 presents the original breathing data and the filtered breathing data obtained using a breathing sensor. The filtered breathing patterns shown in Figs. 7(b) and 8(b) indicate that over the period of 60 s, a total number of 10 breathing cycles were obtained. This comparison also helps to select the specific frequency for detection. It establishes the ability of S-band sensing to successfully record a clear breathing pattern.

To analyze the accuracy of S-band sensing technique, the Sine function fitting algorithm is used to compare the results of the two detecting methods. The procedure of the Sine function fitting algorithm is shown in Fig. 9.

Compared with the breathing sensor, the error of the proposed method can be represented as:

$$E = \frac{|\omega_1 - \omega_2|}{\omega_2} \times 100\% \quad (4)$$

where E is the error of the proposed method. The S-band sensing technique has observed 10 complete breathing cycles. Value of ω_1 is 4.989e−05 for S-band technique, which is equal to b1.

Sine function fitting results for the respiratory sensor in Fig. 10b also have 10 complete breathing cycles with ω_2 = 5.032e−05, which is equal to b1. The error E calculated by Eq. (4) is 0.8%. Comparing the two observations, regardless of intuitive or calculated results, the observations of detecting normal breathing present close agreement. This shows that S-band sensing technique and the designed measurement system have a good ability to detect breathing patterns.

3.2 Sleep apnea detection

Acquisition of the data is in-line with the benchmark study for this part of the experiment. Raw wireless channel information is obtained with the human subject lying

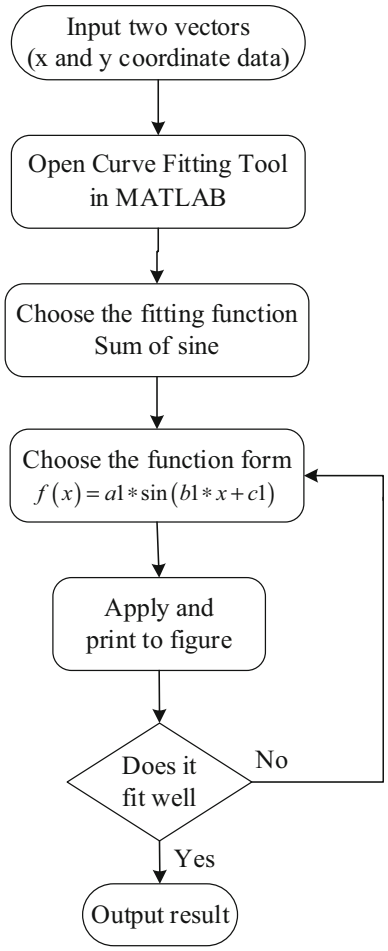

Fig. 9 The flowchart of the Sine function fitting algorithm

straight. The subject first breathes normally, then stops breathing for a while to mimic sleep apnea episode, and then starts breathing normally again. Figure 11 illustrates the raw data for this experiment in 3-D.

Figure 12 shows the breathing pattern observations taken through the respiratory sensor for 120 s duration. The results indicate that the subject is breathing normally from 0 to 52 s. A constant level in amplitude for the next 26 s (from 52nd second to 78th second) reflects that the subject is experiencing a sleep apnea episode. A normal breathing pattern can be observed from the 78th second onward as the apnea episode is over.

S-band sensing results are then analyzed for the sleep apnea measurements. Response for all of the 30 subcarriers is analyzed as shown in Fig. 11. Figure 13a shows the raw variances of amplitude information for subcarrier # 30 over a period of 120 s. The fluctuation of wireless channel information data from 0 to 8 dB indicates the breathing pattern but a sleep apnea episode is not present as clearly as shown in Fig. 13. To reduce the impulse noise, the median filter is applied, obtaining a clear sleep apnea episode from

Fig. 10 Sine function fitting for normal breathing

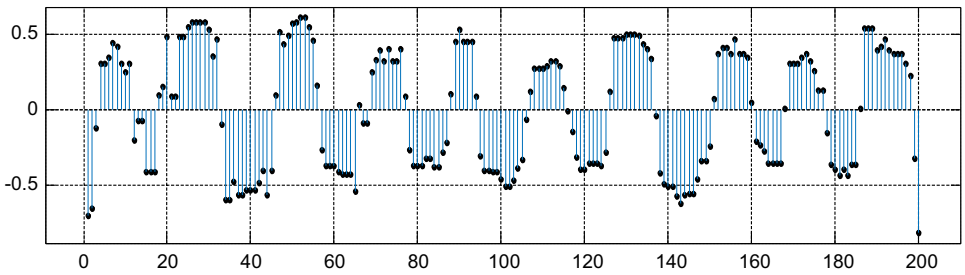

General model Sin1:
f(x) = a1*sin(b1*x+c1)
Coefficients (with 95% confidence bounds:)
a1 = 24.07 (-268.9, 317.1)
b1 = 4.989e-05 (-0.01589, 0.01599)
c1 = 1.762 (-61.01, 64.54)

Goodness of fit:
SSE: 31.72
R-square: 0.001354
Adjusted R-square: -0.008784
RMSE: 0.4013

(a) Normal breathing obtained using S-band sensing technique.

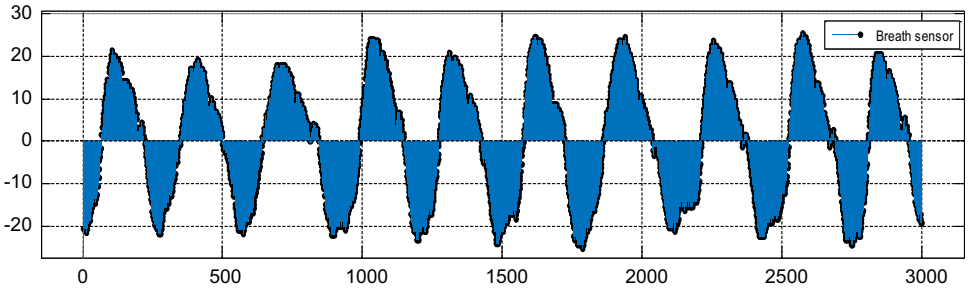

General model Sin1:
f(x) = a1*sin(b1*x+c1)
Coefficients (with 95% confidence bounds:)
a1 = 105.3 (104.5, 106.2)
b1 = 5.032e-05 (-0.0001021, 0.0002028)
c1 = 1.446 (1.304, 1.589)

Goodness of fit:
SSE: 6.856e+05
R-square: 0.000257
Adjusted R-square: -0.0004101
RMSE: 15.12

(b) Normal breathing obtained using breathing sensor.

52nd second to 78th second. This close agreement between the output of the respiratory sensor and S-band sensing further establishes the working of the proposed method as an efficient alternative.

As shown in Fig. 13, the breathing waveform can be approximated as a periodic sinusoidal wave. Hence, the number of the peaks of these sinusoidal waves determines their periodicity and their peak locations ascertain sleep

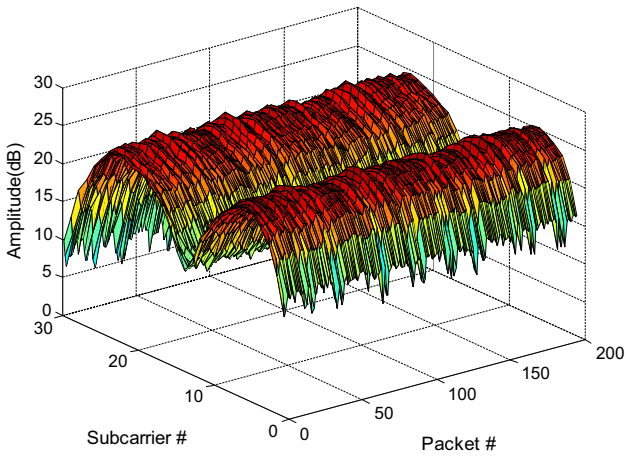

Fig. 11 Raw data recorded for Hypopnea syndrome

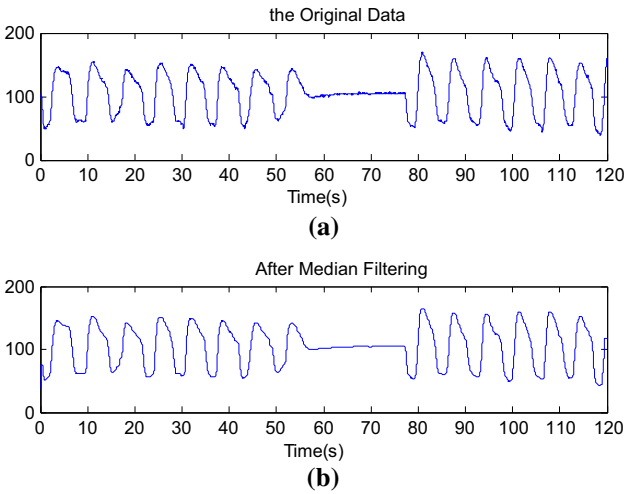

Fig. 12 Sleep apnea detection using breathing sensor

apnea. Thus, we choose peak detection to monitor occurrence of the sleep apnea.

Standard peak detection algorithm is that the maximum is labeled as a peak for every set of three points. For sleep apnea detection, we introduced two changes. First is to set a threshold on the minimum distance between two consecutive peaks. Since the maximal breathing frequency in an adult human is 18 breaths/min, we set a conservative threshold of 3.3 s. Second is to set a threshold on the minimum amplitude at which a peak is detected. We apply the find peaks function in MATLAB to carry out standard peak detection algorithm. The find peaks function is given as follow:

$$[pks, locs] = \text{findpeaks}\Big(\text{data},' \text{MINPEAKDISTANCE}',\ \text{value1},' \text{MINPEAKHEIGHT}', \text{value2}\Big) \tag{4}$$

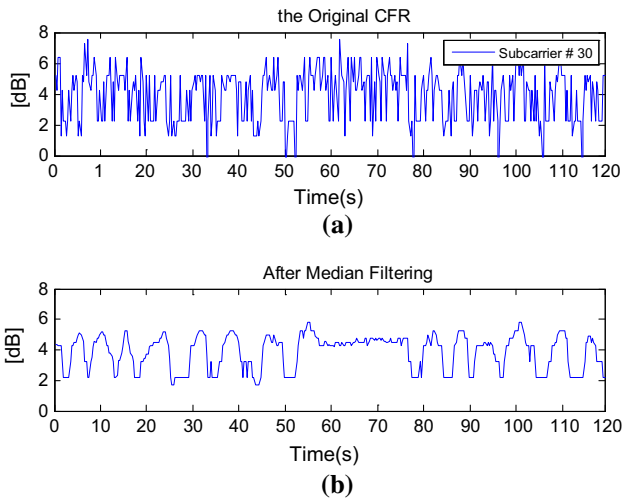

Fig. 13 Variances of amplitude for sleep apnea episode at subcarrier 30

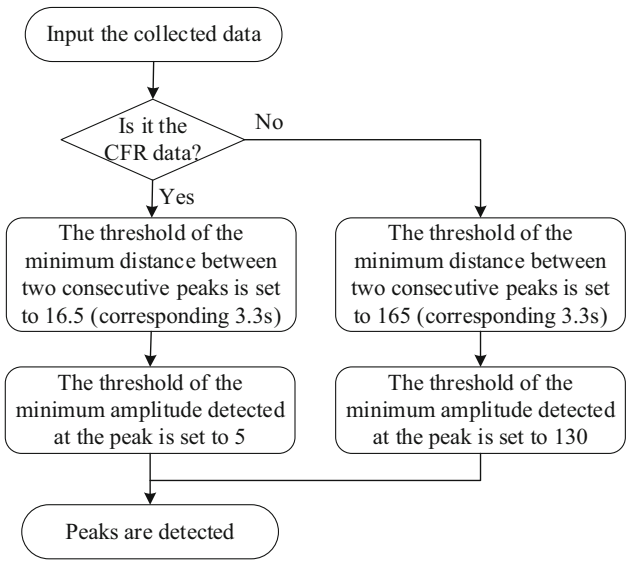

Fig. 14 The flowchart of standard peak detection algorithm

where 'MINPEAKDISTANCE' denotes the threshold of the minimum distance between two consecutive peaks, and the value 1 is set to 16.5 for the CFR data and 165 for the sensor data. 'MINPEAKHEIGHT' represents the threshold of the minimum amplitude detected at the peak, and the value 2 is set to 5 for the CFR data and 130 for the sensor data. Figure 14 shows the flowchart of standard peak detection algorithm.

Figure 15 shows that peak detection algorithm identifies correct peaks and the pause times for the CFR data collected by S-band sensing technique and the respiratory sensor data. The final results can be summarized as follows:

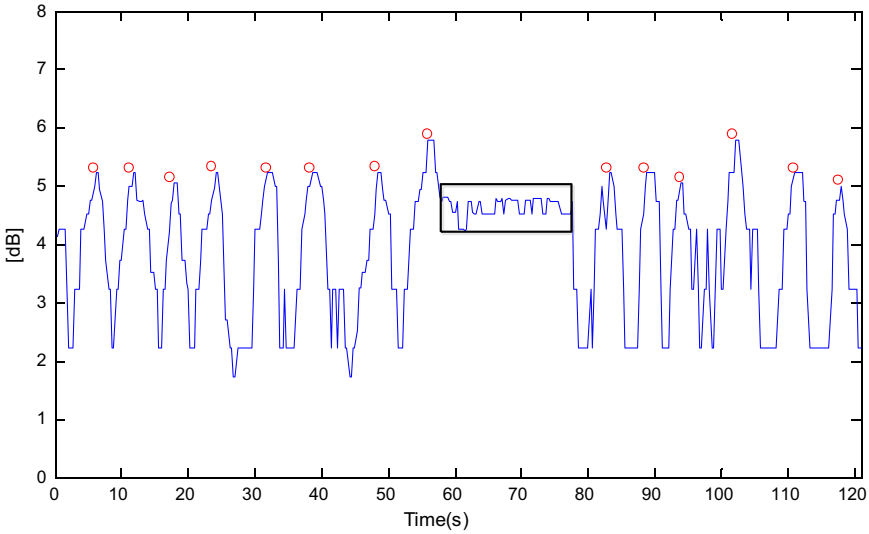

(a) Breathing pattern obtained using S-band sensing technique.

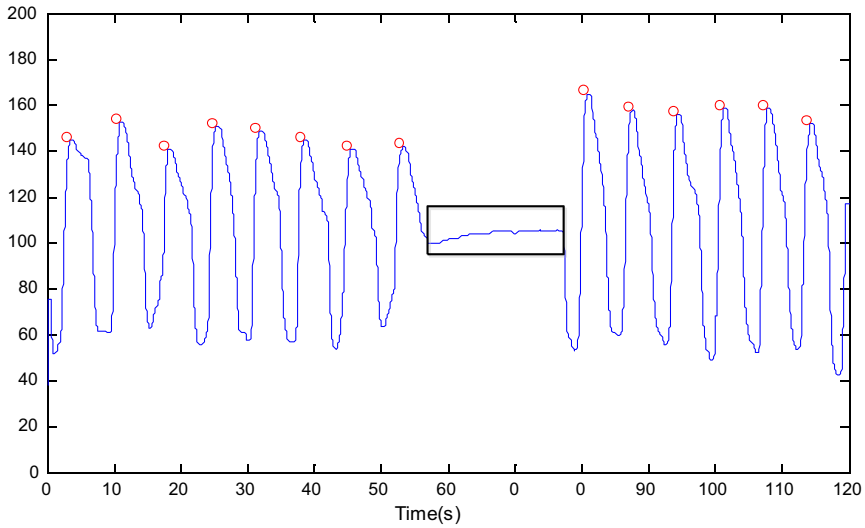

(b) Breathing pattern obtained using breathing sensor.

Fig. 15 Sleep apnea detection using peak detection algorithm

- There are 14 peaks and one apnea in breathing pattern.
- The pause is more than 10 s.
- The results agree with those collected by the respiratory sensor.

We use the Sine function fitting algorithm and peak detection algorithm to process the data collected from all subjects. Except for the results given above from subject 1, the results from subject 3 are shown in Fig. 16. Figure 16a shows the result using the Sine function fitting algorithm, and value of ω_1 is 5.158e−05 for the CFR data and value of ω_2 is 5.674e−05 for the sensor data. The calculated error E is 1.1%. Figure 16b shows that peak detection algorithm identifies correct peaks and the pause times. There are 10 peaks and one apnea for more than ten seconds in one minute, as can be seen in the figure below.

4 Conclusion

A novel contactless monitoring system for breathing pattern observation and sleep apnea detection is presented in this paper. The proposed technique is based on S-band sensing system in an indoor environment and makes use of wireless channel information to observe breathing patterns and identify small changes in the channel response due to the chest movements caused by breathing abnormalities. The proposed system utilizes the median filtering to eliminate impulse noise in the observed data. A detailed measurement campaign is carried out to obtain the breathing pattern of a normal breathing human subject using S-band sensing technique and a standard respiratory sensor simultaneously to compare and establish the working of the proposed technique in benchmark study. Sine function

Fig. 16 The results from subject 3

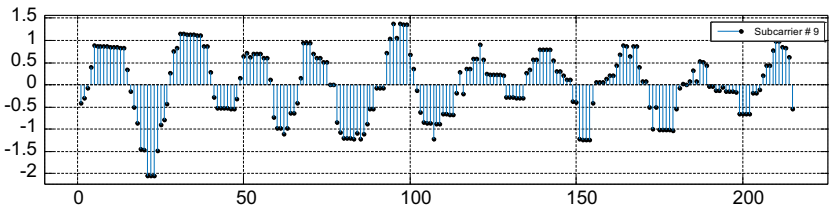

General model Sin1:
f(x) = a1*sin(b1*x+c1)
Coefficients (with 95% confidence bounds:)
a1 = 19.22 (16.35, 23.01)
b1 = 5.158e-05 (-0.0001018, 0.0001081)
c1 = 0.4463 (0.2205, 0.6294)

Goodness of fit:
SSE: 120.8
R-square: 0.000156
Adjusted R-square: 0.0001507
RMSE: 0.7549

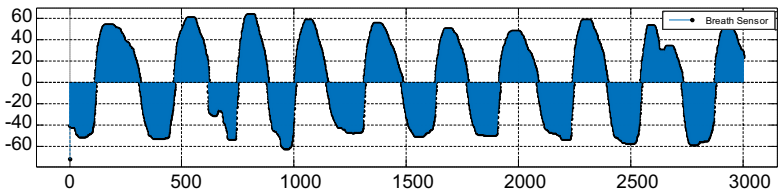

General model Sin1:
f(x) = a1*sin(b1*x+c1)
Coefficients (with 95% confidence bounds:)
a1 = 138 (136.5, 140.2)
b1 = 5.214e-05 (-0.0001106, 0.0002544)
c1 = 0.8426 (0.6304, 0.9689)

Goodness of fit:
SSE: 5.312e-05
R-square: 0.000173
Adjusted R-square: 0.0001066
RMSE: 16.12

(a) The result using the Sine function fitting algorithm

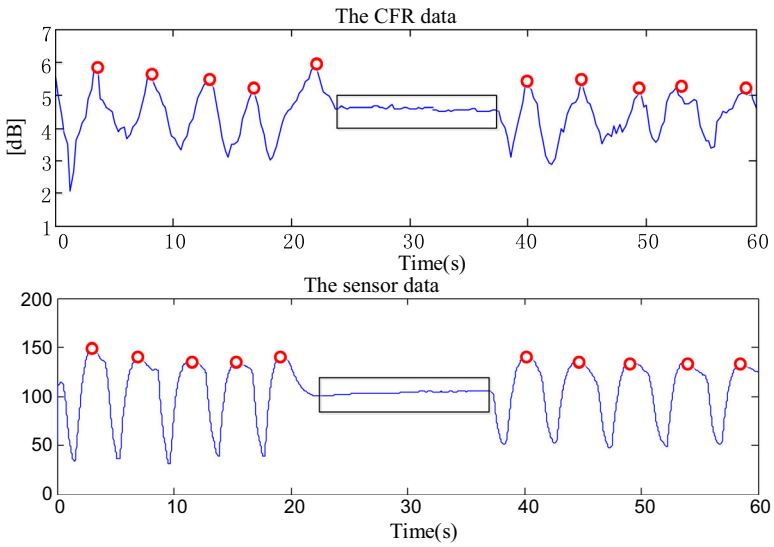

(b) The result using peak detection algorithm.

fitting algorithm is used to analyze the detected results. A close agreement between the two results established the maximum accuracy of the proposed method. The proposed technique is then used to detect Hypopnea syndrome successfully. Similar peaks and pause times using peak detection algorithm observed for the S-band sensing and respiratory sensor for sleep apnea have further established the ability and accuracy of the proposed technique for Hypopnea syndrome detection. The experiment has shown that the proposed S-band sensing is an efficient alternative to traditional Hypopnea syndrome detection methods with added features of contactless, and patient-friendly system exhibiting sufficiently high precision with good potential of early warning Hypopnea syndrome detection for both clinical and home settings. Future work may include multipatients detection, anti-interference diagnosis, etc.

Funding Funding was provided by International Scientific and Technological Cooperation and Exchange Projects in Shaanxi Province (Grant No. 2017KW-005); Fundamental Research Funds for the Central Universities (JB180205); China Postdoctoral Science Foundation funded project (Grant No. 2018T111023); National Natural Science Foundation of China (Grant No. 61301175); National Natural Science Foundation of China (Grant No. 61671349).

Compliance with ethical standards

Conflict of interest The authors declared that they have no conflicts of interest in this work.

References

1. Hoque E, Dickerson RF, Stankovic JA (2010) Monitoring body positions and movements during sleep using WISPs. In: Wireless health 2010, Wh 2010, San Diego, CA, USA, October DBLP, pp 44–53
2. Epstein LJ et al (2009) Clinical guideline for the evaluation, management and long-term care of obstructive sleep apnea in adults. J Clin Sleep Med 5(3):263
3. Erdenebayar U et al (2017) Obstructive sleep apnea screening using a piezo-electric sensor. J Korean Med Sci 32(6):893–899
4. Lee JH, Park HJ, Kim YN (2015) Monitoring obstructive sleep apnea with electrocardiography and 3-axis acceleration sensor, pp 1–6
5. Azimi H, Soleimani Gilakjani S, Bouchard M, Goubran RA, Knoefel F (2018) Automatic apnea-hypopnea events detection using an alternative sensor. In: 2018 IEEE sensors applications symposium (SAS), pp 1–5
6. Morales JF, Varon C, Deviaene M, Borzée P, Testelmans D, Buyse B, van Huffel S (2017) Sleep apnea Hypopnea syndrome classification in SpO_2 signals using wavelet decomposition and phase space reconstruction. In: 2017 IEEE 14th international conference on wearable and implantable body sensor networks (BSN), pp 43–46
7. Vaquerizo-Villar F, Álvarez D, Kheirandish-Gozal L, Gutiérrez-Tobal GC, Barroso-García V, Crespo A, del Campo F, Gozal D, Hornero R (2018) Improving the diagnostic ability of oximetry recordings in pediatric sleep apnea-Hypopnea syndrome by means of multi-class AdaBoost. In: 2018 40th annual international conference of the IEEE engineering in medicine and biology society (EMBC), pp 167–170
8. Casal R, Schlotthauer G (2017) Sleep detection in heart rate signals from photoplethysmography. In: 2017 XVII workshop on information processing and control (RPIC), pp 1–6
9. Salah GB, Abbes K, Abdelmoula C, Masmoudi M (2017) Hypoglossal nerve stimulation in the treatment of obstructive sleep apnea. In: 2017 14th international multi-conference on systems, signals & devices (SSD), pp 429–433
10. Erman MK et al (2007) Validation of the ApneaLink for the screening of sleep apnea: a novel and simple single-channel recording device. J Clin Sleep Med 3(4):387–392
11. Lévy P et al (1996) Accuracy of oximetry for detection of respiratory disturbances in Hypopnea syndrome. Chest 109(2):395
12. Karunajeewa AS, Abeyratne UR, Hukins C (2011) Multi-feature snore sound analysis in obstructive sleep apnea-Hypopnea syndrome. Physiol Meas 32(1):83–97
13. Behar J et al (2013) A review of current sleep screening applications for smartphones. Physiol Meas 34(7):R29–R46
14. Behar J et al (2015) SleepAp: an automated obstructive sleep apnoea screening application for smartphones. IEEE J. Biomed. Health Informat 19(1):325–331
15. Oliver N, Flores-Mangas F (2007) Healthgear: automatic sleep apneadetection and monitoring with a mobile phone. J. Commun. 2(2):1–9
16. Jiang L et al (2012) Automatic sleep monitoring system for home healthcare. In: Proceedings of IEEE-EMBS international conference on biomedical and health informatics, pp 894–897
17. Mack DC et al (2009) Development and preliminary validation of heart rate and breathing rate detection using a passive, ballistocardiography-based sleep monitoring system. IEEE Trans Inf Technol Biomed 13(1):111–120
18. Malakuti K, Albu A (2010) Towards an intelligent bed sensor: Nonintrusive monitoring of sleep irregularities with computer vision techniques. In: Proceedings of international conference on pattern recognition, pp 4004–4007
19. Paalasmaa J et al. (2012) Unobtrusive online monitoring of sleep at home. In: Proceedings of annual international conference on IEEE engineering in medicine and biology society, pp 3784–3788
20. Palmero C et al (2016) Automatic sleep system recommendation by multimodal RBG-depth-pressure anthropometric analysis. Int J Comput Vis 2016:1–16
21. Martinez M et al (2012) Breath rate monitoring during sleep using near-IR imagery and PCA. In: Proceedings of international conference on pattern recognition, pp 3472–3475
22. Wang CW et al (2014) Unconstrained video monitoring of breathing behavior and application to diagnosis of sleep apnea. IEEE Trans Biomed Eng 61(2):396–404
23. Deutsch PA, Simmons MS, Wallace JM (2006) Cost-effectiveness of split-night polysomnography and home studies in the evaluation of obstructive Hypopnea syndrome. J Clin Sleep Med 2:145–153
24. Yang Z, Zhou Z, Liu Y (2013) From RSSI to CSI: indoor localization via channel response. ACM Comput Surv 46(2):25
25. Sudheesh KV, Basavaraj L (2016) Selective weights based median filtering approach for impulse noise removal of brain MRI images. In: International conference on electrical, electronics, communication, computer and optimization techniques (ICEECCOT), IEEE